Bachschmid N., Pennacchi P., Tanzi E. e Vania A.,
"**Identification of Transverse Crack Position and Depth in Rotor Systems**", *Meccanica, International Journal of the Italian Association of Theoretical and Applied Mechanics*, Vol. **35**, n. 6, 2000, CODEN MECCB9 ISSN 0025-6455, pp. 563-582.

IDENTIFICATION OF TRANSVERSE CRACK POSITION AND DEPTH IN ROTOR SYSTEMS

N. BACHSCHMID, P. PENNACCHI, E. TANZI, A. VANIA
Dipartimento di Meccanica – Politecnico di Milano
Via La Masa, 34 - I-20158 Milano, Italy
Fax +39-02.23998492 e-mail nicolo.bachschmid@polimi.it

SOMMARIO

Il presente lavoro illustra un metodo per l'identificazione della posizione e della profondità di una cricca trasversale in un rotore a partire da misure di vibrazione. Come noto da misure in campo e dalla letteratura, la presenza di una cricca trasversale altera il comportamento dinamico del rotore generando in un albero ad asse orizzontale vibrazioni periodiche con componenti 1x, 2x e 3x giro. Un approccio diagnostico basato sul modello del sistema ed un metodo di identificazione mediante il metodo dei minimi quadrati nel dominio delle frequenze vengono utilizzati per la localizzazione della cricca. La profondità della stessa viene invece determinata mediante il confronto tra il momento flettente statico dovuto al peso del rotore ed alle condizioni di allineamento dei cuscinetti ed il momento flettente periodico "equivalente" identificato che simula la presenza della cricca. La validazione del metodo proposto viene quindi effettuata sia staticamente sia dinamicamente mediante risultati sperimentali ottenuti su un test-rig.

ABSTRACT

This paper introduces a method for the identification of the position and the depth of a transverse crack in a rotor system, by using vibration measurements. As it is reported in literature and from field experience, a transverse crack modifies the dynamic behaviour of the rotor, generating in a horizontal axis shaft periodical vibrations with 1x, 2x and 3x rev. components. A model based diagnostic approach and a least squares identification method in the frequency domain are used for the crack localisation along the rotor. The crack depth is calculated by comparing the static bending moment, due to the rotor weight and to the bearing alignment conditions, to the identified "equivalent" periodical bending moment, which simulates the crack. Finally, the validation of the proposed method is carried out statically and dynamically by means of experimental results obtained on a test-rig.

Keywords: *Cracks, Identification, Rotating shafts, Vibrations.*

INTRODUCTION

Propagating transverse cracks have been discovered in the last 20 years [1] in several rotors of steam turbines or generators of European power plants. Fortunately, as far as the authors know, they have been detected before the crack had propagated to a critical depth, that means before the occurrence of a catastrophic failure. The cracked rotors have then been removed and inspected and spare rotors could generally be installed, limiting this way the damage to the cost of the rotor and of the loss of production only during overhaul.
In many cases however the crack had propagated to a depth of 50% of the diameter, in some cases up to 75%. In these situations only 50% or about 20% respectively of the cross sectional area was

left for transmitting forces and moments. Due to the rapidly increasing crack propagating rate, probably a catastrophic failure with a possible total damage of the plant would have occurred, within only few hours or days of operation at full speed.

The importance of early detection of cracks, possibly by means of an automatic diagnostic methodology instead of a vibration specialist's expertise, appears obvious from these considerations.

Many authors have studied the dynamic behaviour of rotors with transverse crack (an extensive survey is given in [2] and a recent contribution is in [3]) and therefore the symptoms of a cracked rotor are well known: a change in 1x rev., 2x rev. and 3x rev vibration vector (amplitude and phase) is suspect. In fact the presence of a crack and its propagation determine a local reduction of the rotor stiffness along with a change in the rotor natural frequencies. A change in natural frequency depending on the angular position of the rotor is a symptom of a crack, but this change is generally small and difficult to detect. Actually this phenomenon is rather complicate, since during the rotation the crack "breaths", i.e. the mechanism of opening and closing of the crack is ruled by the stress acting on the cracked section due to the external loads; in a rotor the stress are time depending with a period equal to the period of rotation, thus the crack "periodically breaths". However, 1x rev. components can be caused by many other faults (e.g. unbalance, bow, coupling misalignments) and 2x rev. components can be due also to polar stiffness asymmetries (in generators), to surface geometry errors (journal ovalization) and to non-linear effects in oil film bearings. These two last causes can also generate 3x rev. components.

Therefore, it is not easy to attribute these symptoms with certainty to a developing crack. Furthermore when the developing crack is in an early stage, the changes in vibration are generally so small and masked by noise that they are difficult to be detected from the bearing measurements. Finally, it is worth noting that also the position of the crack strongly influences the change of the vibration. Only for cracks in positions along the shaft line in which high static bending moments act (due to weight and bearing reaction forces), the generated vibrations in the bearings are consistent. When the bending moment in correspondence of the crack is small, also the resulting vibrations are small and might be unrecognisable.

Fortunately another symptom helps to identify a crack: that is the thermal behaviour. During a heating transient of the surrounding fluid (e.g. steam in a steam turbine or cooling gas in a generator) the outer surface, the "skin", of the rotor has a higher temperature, with respect to the mean temperature; this causes elongation and compressive stresses which force the crack to close: the crack is prevented from breathing or the breathing is reduced. As a consequence, the crack induced 1x rev. and 2x rev. components are reduced.

A cooling transient effects tensile stresses in the skin, which force the crack to open: the rotor bows, a change in 1x rev. component appears due to the bow, and an increase in 2x rev. component appears due to the crack, which could be held completely open by the tensile stresses. Also in this case the crack is prevented from breathing or the breathing is anyhow reduced. These symptoms during thermal transients allow the identification of the transverse crack with certainty. In two different turbogenerator groups in Italian power plants, the transverse crack in a HP steam turbine and in a 320 MW generator could be detected thanks to this particular thermal sensitivity.

Once the type of fault has been identified in a shaft line, also its most probable position and its depth should be identified. The first task can be accomplished by means of the least square approach in the frequency domain, which is described in the next paragraph, while the proposed method for the depth identification is introduced in the following. Finally, dynamic and static tests are used to validate the proposed method.

THE IDENTIFICATION METHOD

The identification procedure can be performed as usual by means of causality correlations of measurable symptoms to the faults. Two main approaches can be used, as described in [4]. In the first approach, the symptoms can be defined using qualitative informations, based on human operators' experience, which creates a knowledge base. An expert system can then be built up in which different diagnostic reasoning strategies can be applied. Fault-symptom matrices, fault-symptom trees, if-then rules or fuzzy logic classifications can be used to indicate in a probabilistic approach the type, and sometimes also the size and the location of the most possible fault. Also artificial neural networks (ANN) can be used for creating the symptom-fault correlation. This qualitative diagnostic approach is widely used both in industrial environments and in advanced research work.

A different approach is the so-called model based fault detection method. In this case a reliable model of the system or of the process, is used for creating the symptom-fault correlation, or the input-output relation. The fault detection can then be performed by means of different approaches, according to the nature of the system under observation:

- parameter estimation, when the characteristic constant parameters of the process, or of the components are affected by the fault.
- state estimation , when the constant parameters are unaffected by possible faults, and only the state of the system, which is represented by a set of generally unmeasurable state variables (function of time), is affected by the faults; in this case the model acts as a state observer.
- parity equations, when the faults affect some of the unmeasurable input variables, the parameters are constant, and only output variables are measured and compared with calculated model output variables.

Therefore, the fault can be identified from parameter or state estimation or from parity equations.

This last approach is used in the model based identification procedure described in this paper in which the input variables are the exciting forces and the output variables are the vibrations; the procedure requires the model definition of the elements (rotors, bearings, supporting structure) that compose the rotor system. A finite beam element model is assumed for the rotor, the bearings are represented by means of their stiffness and damping matrices (therefore non-linear oil film effects are neglected), while several representation can be given for the foundation, such as modal, elasto-dynamic matrix or lumped springs and dampers.

Also the effect of the faults has to be modelled and this is done by introducing an equivalent system of external forces and moments. In fact, in the parameter estimation approach, the identification of the changes in the system parameters (such as the stiffness of the rotor system in the case of the crack) seems to be a more difficult task than the identification of the equivalent external forces, because the system parameters influence generally the complete mass, stiffness and damping matrices of the system. In other words, with reference to the standard matrix equation of the system

$$\mathbf{M}\,\ddot{\mathbf{x}}_t + \mathbf{D}\,\dot{\mathbf{x}}_t + \mathbf{K}\,\mathbf{x}_t = \mathbf{F}(t) \tag{1}$$

it seems difficult to identify the changes in the matrices **M**, **D**, and **K** from measurement of vibration $\mathbf{x}_t$, in only few measuring points along the shaft, such as occurs in real machines. Let's indicate by $d\mathbf{M}$, $d\mathbf{D}$ and $d\mathbf{K}$ the changes in mass, damping and stiffness matrices due to system parameter changes caused by the developing fault. Eq. (1) yields:

$$\left(\mathbf{M} + d\mathbf{M}\right)\ddot{\mathbf{x}}_t + \left(\mathbf{D} + d\mathbf{D}\right)\dot{\mathbf{x}}_t + \left(\mathbf{K} + d\mathbf{K}\right)\mathbf{x}_t = \mathbf{W} + \left(U + M_u\right)e^{i\Omega t} \tag{2}$$

in which the r.h.s. external forces $\mathbf{F}(t)$ are generally unknown, because they are composed by the weight (which is known) and by the original unbalance and bow (which are unknown). Despite the fact that the crack behaviour is influenced also by the vibrations experienced by the rotor, which make the system non-linear, in horizontal heavy rotors the crack behaviour is dominated by the static deflection due to the weight, so that the non-linearity can be neglected. If the system is considered to be linear, then the vibration $\mathbf{x}_t$ can be considered to be split in two parts which can be simply superposed:

$$\mathbf{x}_t = \mathbf{x}_1 + \mathbf{x} \tag{3}$$

The first vibration vector ($\mathbf{x}_1$) is due to the weight $\mathbf{W}$ and the unknown unbalance force $U\, e^{i\Omega t}$ and unbalance moment $M_u\, e^{i\Omega t}$, and the second ($\mathbf{x}$) is due to the developing fault. The component $\mathbf{x}$ may be obtained by calculating the vector differences of the actual vibrations (due to weight, original unbalance and fault) minus the original vibrations measured, in the same operating conditions (rotation speed, flow rate, power, temperature, etc.) before the fault was developing. Recalling the definition of $\mathbf{x}_1$, the pre-fault vibration, the following equation holds:

$$\mathbf{M}\,\ddot{\mathbf{x}}_1 + \mathbf{D}\dot{\mathbf{x}}_1 + \mathbf{K}\,\mathbf{x}_1 = \mathbf{W} + \left(U + M_u\right) e^{i\Omega t} \tag{4}$$

which substituted in eq. (2) gives:

$$\mathbf{M}\,\ddot{\mathbf{x}} + \mathbf{D}\dot{\mathbf{x}} + \mathbf{K}\,\mathbf{x} = -d\mathbf{M}\,\ddot{\mathbf{x}}_t - d\mathbf{D}\dot{\mathbf{x}}_t - d\mathbf{K}\,\mathbf{x}_t \tag{5}$$

The r.h.s. of eq. (5) can be considered as a system of equivalent external forces which force the fault-free system to have the change in vibration defined by $\mathbf{x}$ that is due to the developing fault only:

$$\mathbf{M}\ddot{\mathbf{x}} + \mathbf{D}\dot{\mathbf{x}} + \mathbf{K}\,\mathbf{x} = \mathbf{F}_f(t) \tag{6}$$

Using this last approach, the problem of fault identification is then reduced to a force identification procedure with known system parameters. Keeping in mind that the final goal is the identification of faults, this approach is preferred since only few elements of the unknown fault forcing vector are in reality different from zero, which reduces sensibly the number of unknowns to be identified. Infact the fault forces are considered to be applied in not more than two different nodes along the rotor. If we consider a steady-state situation, assuming linearity of the system and applying the harmonic balance criteria from eq. (6), we get, for each harmonic component, the equations

$$\left[-(n\Omega)^2\,\mathbf{M} + i\,n\Omega\,\mathbf{D} + \mathbf{K}\right]\mathbf{X}_n = \mathbf{F}_{f_n} \tag{7}$$

where the force vector $\mathbf{F}_{f_n}$, has to be identified. Few spectral components in the frequency domain (generally not more than 3) $\mathbf{X}_n$ measured in correspondence of the bearings, represent completely the periodical vibration time history. Moreover, the fault acts on few d.o.f. of the system, so the vector $\mathbf{F}_{f_n}$ is not a full-element vector which is convenient to be represented by means of a complex value $\overline{A}$ and a localisation vector [$\mathbf{F}_L$]: e.g. the complex vector, which models the unbalance has only the 1x rev. component and the following representation:

$$\mathbf{F}_{f_1} = \begin{bmatrix}0 & \vdots & 1 & 0 & i & 0 & \vdots & 0\end{bmatrix}^{\mathrm{T}} \cdot mr\Omega^2 e^{i\varphi} = [\mathbf{F}_L]\,\overline{A} \tag{8}$$

where the only elements different from zero are the ones relative to the horizontal and vertical d.o.f. of the node j, where the unbalance is supposed to be applied. Further details about the model of the faults are reported in [5].

In the case of a transverse crack the approach according eq. (5) is convenient, where only $d\mathbf{K}$ is different from zero. It has been shown [6] that a crack can be modelled by a suitable system of external forces or couples, which depend on the depth of the crack and of the bending moment which is applied to the rotor in the cracked section. Due to the "breathing" mechanism of the crack during the rotation, the stiffness matrix is periodic and its Fourier expansion can be truncated at the third harmonic component.

$$\mathbf{K}(\Omega t) = \mathbf{K}_m + \Delta\mathbf{K}_1 e^{i\Omega t} + \Delta\mathbf{K}_2 e^{i2\Omega t} + \Delta\mathbf{K}_3 e^{i3\Omega t} \tag{9}$$

The average term $\mathbf{K}_m$ then appears at the l.h.s. of eq. (7), while the other terms generate 1x rev., 2x rev. and 3x rev. forces on the r.h.s. of eq. (7), which can be rewritten in the following form, using an harmonic balance approach:

$$\left[-(n\Omega^2)\mathbf{M} + i\,n\Omega\mathbf{D} + \mathbf{K}_m\right]\mathbf{X}_n\, e^{in\Omega t} = -\Delta\mathbf{K}_n e^{in\Omega t}\left(\mathbf{X}_{st} + \mathbf{X}_n\, e^{in\Omega t}\right) \quad n = 1, 2, 3 \tag{10}$$

The equivalent force system (on the r.h.s. of eq. (10)) is applied to the two nodes of the element which contains the crack and is therefore composed by a vector of eight generalized forces (in case of 4 d.o.f. per node model). Among these forces it results from energy considerations that the most important are the bending moments which are rotating and roughly equal and opposite on the two nodes. Therefore the unknowns are reduced to one bending moment M_n only for each harmonic component. The localisation vector $[\mathbf{F}_L]$ and $\overline{A}$ have the following expressions:

$$\left[\mathbf{F}_L\right] = \left[0 \;\; \vdots \;\; 0 \;\; i \;\; 0 \;\; 1 \;\; 0 \;\; -i \;\; 0 \;\; -1 \;\; \vdots \;\; 0\right]^{\mathrm{T}} \qquad \overline{A}(n) = M_n\, e^{in\varphi}, \quad n = 1, 2, 3 \tag{11}$$

Now eq. (7) can be rewritten, for each harmonic component, in the following way:

$$\left[\mathbf{E}(n\Omega)\right]\mathbf{X}_n = \mathbf{F}_{f_n} \tag{12}$$

where $\left[\mathbf{E}(n\Omega)\right]$ is the system dynamic stiffness matrix for the speed Ω and for the n^{th} harmonic component. This matrix can be inverted and eq. (12) becomes

$$\mathbf{X}_n = \left[\mathbf{E}(n\Omega)\right]^{-1} \cdot \mathbf{F}_{f_n} = \boldsymbol{\alpha}_n \cdot \mathbf{F}_{f_n} \tag{13}$$

where $\boldsymbol{\alpha}_n$ is the inverse of $\left[\mathbf{E}(n\Omega)\right]$. Reordering in a opportune way the lines in eq. (13), by partitioning the inverse of the system dynamic stiffness matrix, we obtain:

$$\begin{cases} \mathbf{X}_{B_n} = \boldsymbol{\alpha}_{B_n} \cdot \mathbf{F}_{f_n} \\ \mathbf{X}_{A_n} = \boldsymbol{\alpha}_{A_n} \cdot \mathbf{F}_{f_n} \end{cases} \tag{14}$$

where $\mathbf{X}_{B_n}$ is the complex amplitude vector representing the measured absolute vibrations in correspondence of the bearings and $\mathbf{X}_{A_n}$ is the vector of the remaining d.o.f. of the rotor system model.

Using the first set of Eqs. (14), the differences $\boldsymbol{\delta}_n$, between calculated vibrations $\mathbf{X}_{B_n}$ and measured vibrations $\mathbf{X}_{Bm_n}$ can be defined, for each harmonic component, as:

$$\boldsymbol{\delta}_n = \mathbf{X}_{B_n} - \mathbf{X}_{Bm_n} = \boldsymbol{\alpha}_{B_n} \cdot \mathbf{F}_{f_n} - \mathbf{X}_{Bm_n} \tag{15}$$

The number of equations n_E (number of measured d.o.f.) is lower than the number n_F (number of d.o.f. of the complete system model) which is also the number of elements of $\mathbf{F}_{f_n}$. But, as said before, $\mathbf{F}_{f_n}$ becomes a vector with many null-elements so that the number of unknown elements of $\mathbf{F}_{f_n}$ is smaller than the number of equations. The system therefore has not a single solution for all the equations and we have to use the least square approach in order to find the solution (identified fault) that minimise the differences which are calculated for all the different rotating speeds which are taken into consideration.

A scalar relative residual may be defined by the root of the ratio of the squared $\boldsymbol{\delta}_n$, divided by the sum of the squared measured vibration amplitudes $\mathbf{X}_{Bm_n}$:

$$\delta_{r_n} = \left(\frac{\left[\boldsymbol{\alpha}_{B_n} \cdot \mathbf{F}_{f_n} - \mathbf{X}_{Bm_n}\right]^{\mathrm{T}} \left[\boldsymbol{\alpha}_{B_n} \cdot \mathbf{F}_{f_n} - \mathbf{X}_{Bm_n}\right]}{\mathbf{X}_{Bm_n}^{\mathrm{T}} \, \mathbf{X}_{Bm_n}} \right) \tag{16}$$

By means of the hypothesis of localisation of the fault, the residual is calculated for each possible node of application of the defect.

Where the residual reaches its minimum, there is the most probable position of the fault. The relative residual gives also an estimate of the quality of the identification, since it results the closer to zero the better the identified fault corresponds to the actual one; this follows easily from the analysis of the numerator of eq. (16).

In the case of the crack, it is worth noting that the 1x rev. vibration components are due both to the breathing mechanism of the crack and to a local bow that generally has developed during the crack propagation. Therefore, when no other sources of bow are present, the 1x rev. component is useful for the localisation of the crack, but not for the identification of its depth.

The 3x rev. component is rather small and generally masked by some noise. Often this component can be recognised only when approaching the resonant condition at a rotating speed equal to 1/3 the rotor’s critical speed. This may be an interesting symptom of the presence of a crack, but is generally insufficient for identfying its position and depth.

The 2x rev. component is therefore the most suitable symptom for detecting position and depth of the crack; the highest values are obviously reached during a run-down transient when approaching the resonant condition at 1/2 critical speed.

IDENTIFICATION OF THE CRACK DEPTH

Let’s consider now the beam element in which the presence of a crack has been identified as most probable (with the lowest relative residual): the least square approach provides also the values of the equivalent bending moments M_1, M_2 and M_3 from corresponding 1x, 2x and 3x rev. measured vibration components.

Then the static bending moment M in correspondence of the same element, due to the weight and to bearing alignment conditions, is calculated from model data. Defining p the relative depth of the crack with rectilinear tip, according to Figure 1, in [4,5] it has been shown that the ratio of the nx rev. equivalent bending moment M_n to the static bending moment M is a function of the relative depth p only.

This is represented in Figure 2 for the 1x, 2x and 3x rev. component and expressed by the relationship in eq. (17).

$$\frac{M_n}{M} = f(p) \tag{17}$$

In Figure 2 also the ratio for the 2x rev. component in the case of a always open (non “breathing”) crack, which can be considered a slot, is shown.

This relationship has been obtained by analysing the breathing behaviour of cracks with rectilinear tips, as that one shown in Figure 1, in rotors in steady state thermal conditions. Different shapes will cause slightly different behaviours. The presence of a thermal transient that influences the “breathing” mechanism, will also cause different behaviours.

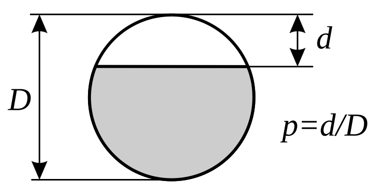

Figure 1 Crack with rectilinear tip.

Eq. (17) can then be used for determining the crack depth, under the assumption that the crack has a rectilinear tip and that the rotor is in steady state thermal condition. But, as shown in [5], the length l_c of the "equivalent", reduced stiffness, beam element that simulates the behaviour of the cracked beam, is also depending on the relative crack depth p:

$$\frac{l_c}{D} = g(p) \tag{18}$$

The function $g(p)$ is represented in Figure 4.

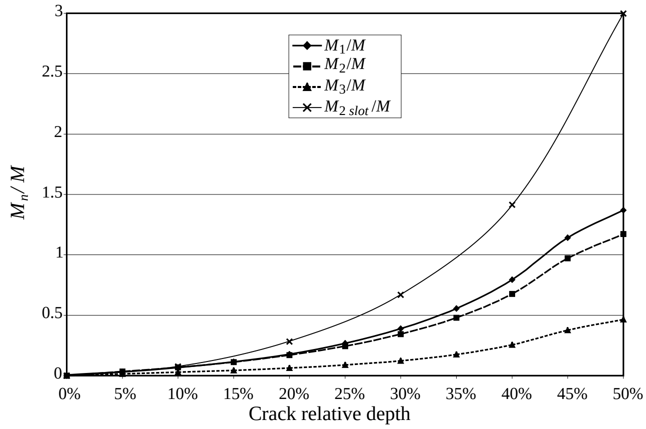

Figure 2 Ratio of the bending moments on the equivalent cracked beam, as a function of crack relative depth.

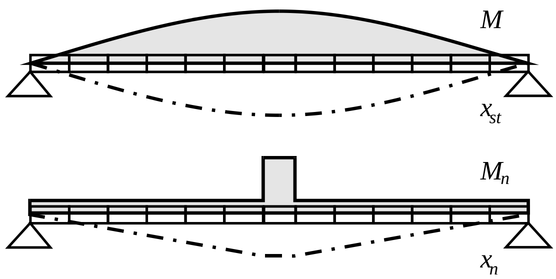

Figure 3. Typical bending moments and deflections for a symmetrical rotor on 2 bearings, with a crack at mid span.

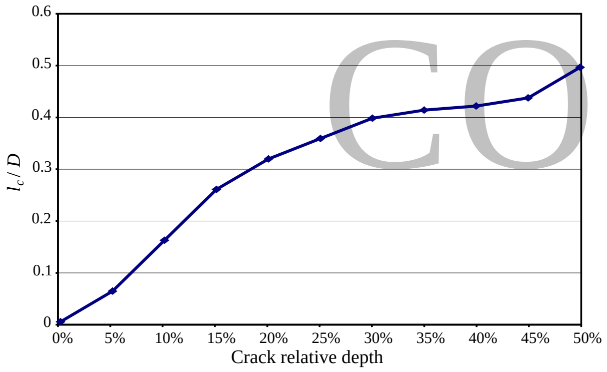

Figure 4. Relationship between the crack relative depth p, the diameter *D* and the length l_c of "equivalent" beam.

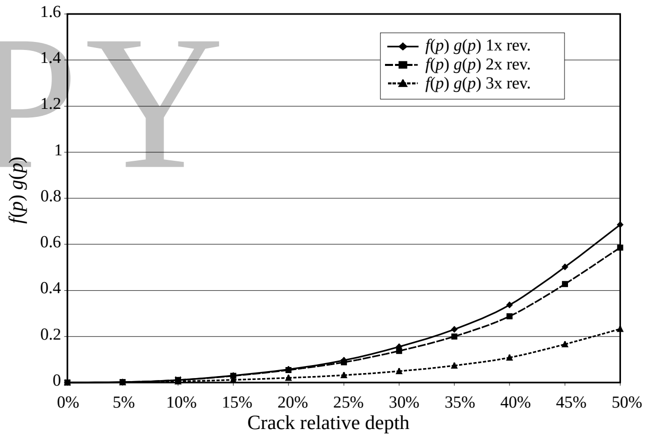

Figure 5. Function for the calculation of the crack depth.

Now we have the equivalent bending moments M_n which are applied to an element with a wrong length: l instead of l_c. It is worth noting that the nx rev. measured displacements are due to the relative rotation of the cracked element extremity nodes, which is proportional to the product $M_n \cdot l$ of the identified nx rev. bending moment component applied to one element of the f.e. model of the rotor, multiplied by its length.

The equivalent bending moment component M'_n, applied to an equivalent cracked beam element of length l_c, can therefore be calculated by imposing some relative rotation, as:

$$M'_n \cdot l_c = M_n \cdot l \tag{19}$$

By assuming that the static bending moment M applied to the original element of length l does not change much along the element (see e.g. Figure 3 in which typical bending moments and related

deflections are represented), the same M can be considered applied to the element with equivalent length l_c.
Recalling eq. (17) we can derive:

$$\frac{M'_n}{M} = \frac{M_n \cdot l}{M \cdot l_c} = f(p) \tag{20}$$

and using eq. (18) we get:

$$\frac{M_n \cdot l}{M \cdot D} = f(p) \cdot g(p) \tag{21}$$

Eq. (21), shown in Figure 5 for the 1x, 2x and 3x rev. components and the 2x rev. slot, can then be used for determining, from the known left hand side, the relative depth of the crack.

EXPERIMENTAL TESTS

Test rig description

The MODIAROT test rig, shown in Figure 6, is composed by two rigidly coupled rotors, supported on four lemon shaped oil film bearings, driven through a flexible coupling by a variable speed inverter controlled electric motor. The shaft diameter is 25 mm and the total length of the two rigid coupled shafts is about 2 m, the total mass is less than 100 kg. The critical speeds are around 1200 rpm (1st) and 3400 rpm (2nd). The supporting structure is flexible and has several natural frequencies in the operating speed range (a resonance is around 2000 rpm). The vibrations in each bearing are measured by 2 eddy-current proximity probes fixed to the bearing housing in ±45° directions with respect to the vertical, measuring the shaft relative displacements. Each bearing housing is equipped with 2 accelerometers measuring the absolute vibrations of the bearing housing. By rotating the reference frame and adding the absolute displacement of the bearing housing, the absolute vibrations of the shaft in correspondence of the bearing can be obtained and compared with calculated results. All signals during a run-down transient were analyzed by a 8 channel spectrum analyzer in tracking filter modality. This heavy processing of the experimental data introduced significant errors in the experimental data, as will be shown later.

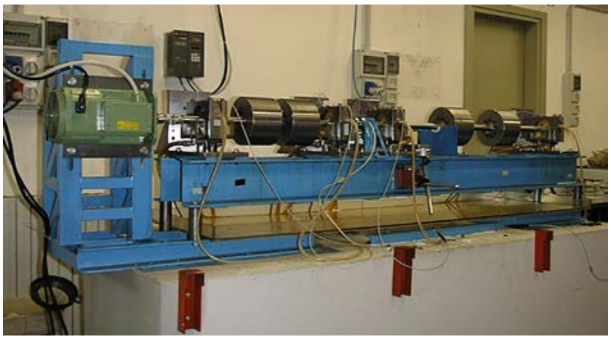

Figure 6. 4-bearing 2-shaft MODIAROT test rig on flexible foundation with fully instrumented bearing housing.

A crack with estimated depth ranging from 25% to 30% of the shaft diameter has been generated by means of fatigue bending solicitation in the middle of the longer shaft, starting from a very small slot (Figure 7). The tests have been carried out on both the quasi-static and the dynamic behaviour. In the first case, the longer shaft has been disassembled and positioned on supports or on a lathe.

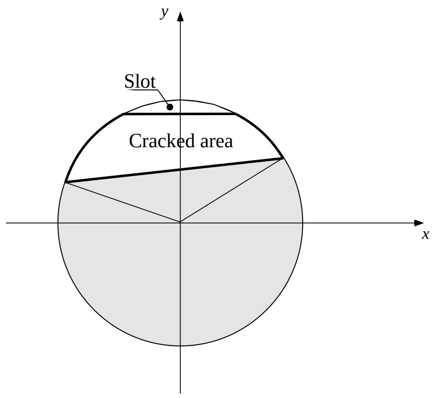

Figure 7. Supposed crack profile.

Natural frequencies

Different values of natural frequencies should be found in cracked rotors, depending on its angular position and therefore on the "open" or "closed" situation of the crack.

The frequencies corresponding to a complete open crack and to a complete closed crack have been calculated, assuming a stiff supporting structure and measuring its natural frequencies with impact tests, in the configuration shown in Figure 8 and Figure 9.

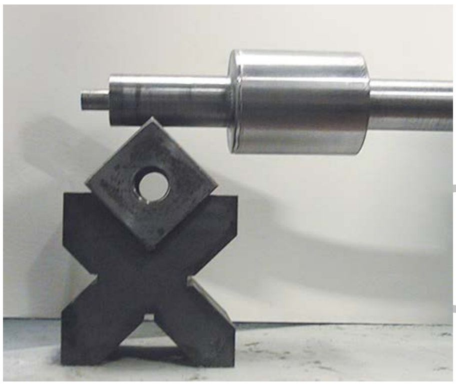

Figure 8 Experimental simulation of the ideal support (particular of an extreme of the shaft).

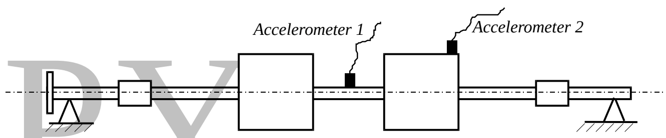

Figure 9 Shaft position on the two supports and location of the accelerometers.

Table 1 summarises the comparison between the experimental results and the frequencies calculated with the model proposed in [6]. The agreement is rather good, giving a first confirmation to the validity of the proposed model.

Crack	Experimental		Calculated (25%)		Calculated (30%)	
	1st	2nd	1st	2nd	1st	2nd
Closed	12.725	59	12.30	59.04	12.30	59.04
Open	12.425	59	12.14	59.04	12.06	59.04

Table 1 - Natural frequencies (in Hz) of the 1st and 2nd modes.

The experimental values, which were measured with a resolution of ±0.025 Hz, show a variation in natural frequencies of roughly 2.3%. The calculated values instead have a variation of 1.30% for 25% depth and 1.93% for 30% depth. No variation at all has been found for the 2nd mode since the crack, located in correspondence of the node of the mode shape, does not affect its bending stiffness (or modal stiffness).

Quasi-static Behaviour

The cracked shaft, equipped with its massive disks, was mounted on a lathe and 4 proximity probes have been installed according to Figure 10 on a movable frame. The sensor signals have been recorded during slow rotation in 11 positions along the shaft and analysed.

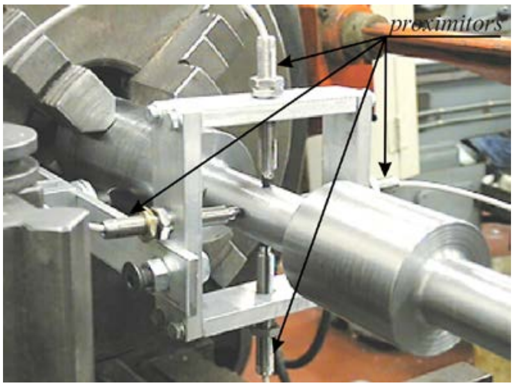

Figure 10. Proximitor arrangement on the PdM test rig.

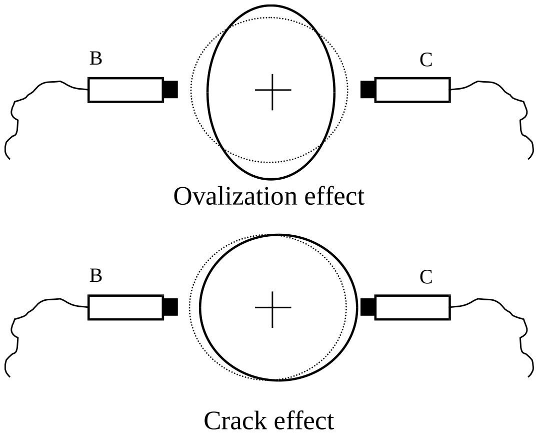

Figure 11. 2x rev. components.

The sensors in opposite positions allow to separate 2x rev. component geometric errors (shaft ovalization) from 2x rev. component due to the crack: the sum indicates twice the ovalization, the difference twice the 2x rev. displacement (Figure 11).

The vertical and horizontal 2x rev. should be equal, according to the results of the model as exposed in [6]. The measured displacements have been compared with those calculated with the simplified model, for a depth of 24%: these comparisons are shown in Figure 12 and Figure 13 for the horizontal and vertical components. The 2x rev. measured deflection is rather linear, except for the small cracked element, and fits very well with the calculated deflection.

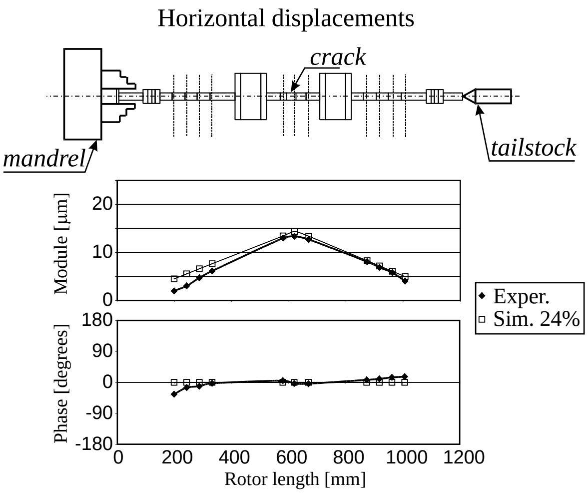

Figure 12 2x rev. component in horizontal direction due to the crack. Comparison between experimental and calculated results.

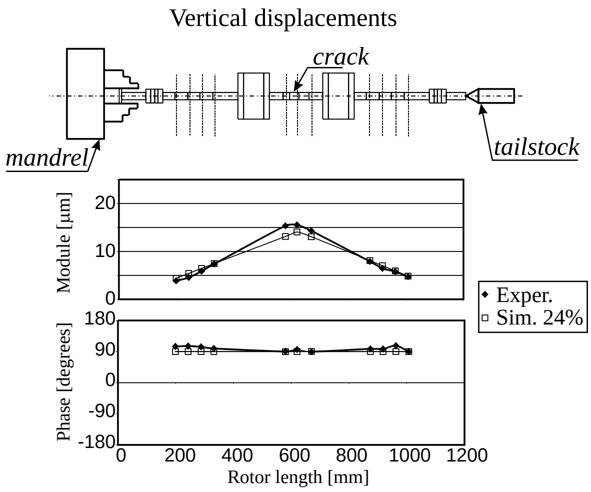

Figure 13 2x rev. component in vertical direction due to the crack. Comparison between experimental and calculated results.

These results validate the model of the “breathing” mechanism, the model of the equivalent beam and the calculation procedure proposed in [6].

With regard to the other harmonic components, the 1x rev. component is masked by a high static bow, while the 3x rev. component is so small that its presence is masked by geometric surface errors and by the measuring errors.
The displacement values of the 2x rev. components, for all the 11 measuring points, have been used for the identification procedure. The results obtained are shown in Figure 14.
The location of the suspected crack is identified with good accuracy, and also its depth is identified. The high quality of the identification is measured by the low value of the residual ($\delta = 0.182$). The good identification results are probably due to the high number of measuring stations (11), which allows to define very well the deflection shape.

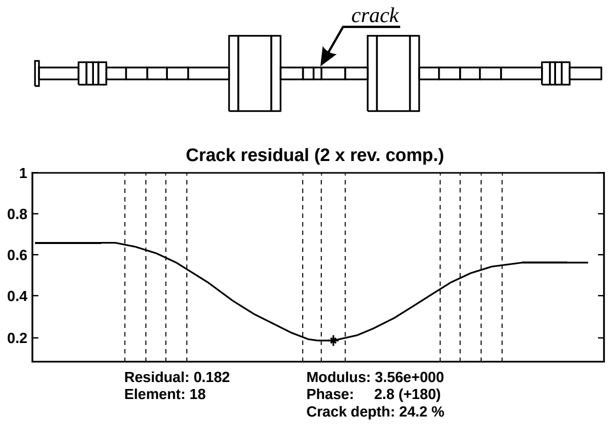

Figure 14 Crack identification in quasi-static case.

Dynamic Behaviour

The same cracked shaft, installed in the test rig, shows at low speed vanishing small 2x rev. components in the bearings, which are completely masked by 2x rev. ovalization errors in the shaft journals.
The experimental results obtained in the bearings (e.g. in bearing 3) are shown in Figure 15 for the 1x rev. component, where a high bow is recognisable, in Figure 16 for the 2x rev. component, where a high ovalization error is recognisable and in Figure 17 for the 3x rev. component, where the amplitude of 2 μm is exceeded only when passing through a resonance.

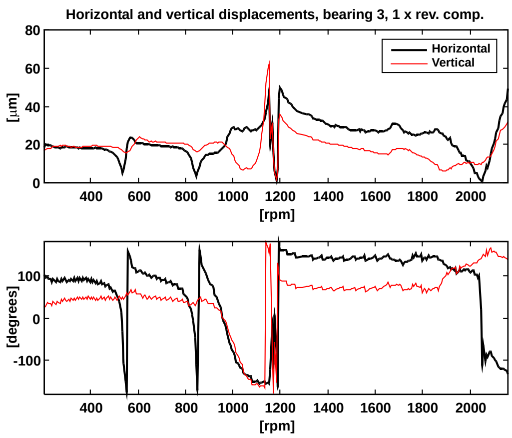

Figure 15 Experimental displacements at bearing 3, 1x rev. component of cracked shaft.

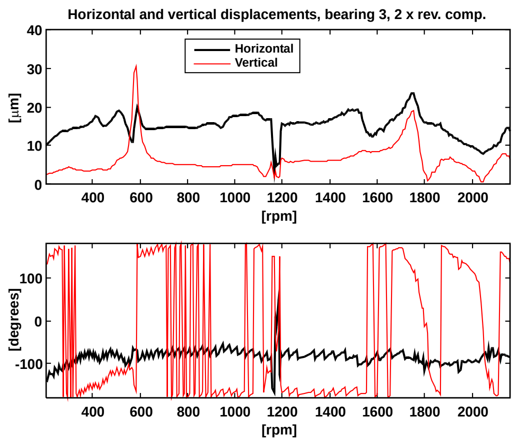

Figure 16 Experimental displacements at bearing 3, 2x rev. component of cracked shaft.

The previously stored 2x rev. components of the uncracked rotor have been subtracted from the actual vibrations and the 2x rev. vibration differences are represented in Figure 18. It can be seen that the crack induced 2x rev. components in the bearings are affected by errors due to the heavy processing of the experimental data. Also the data below 550 rpm were lost.

In order to emphasise the vibrations due to the crack, a measuring station with four proximity probes, similar to that one of Figure 10, has been positioned in correspondence of the crack. The results in terms of 2x and 3x rev. components in vertical direction are shown in Figure 19 and Figure 20. The agreement with calculated results is much better in this measuring station with respect to the measuring stations taken in the bearings (not shown for lack of space). In this case the data have not been processed, nor vector differences have been made.

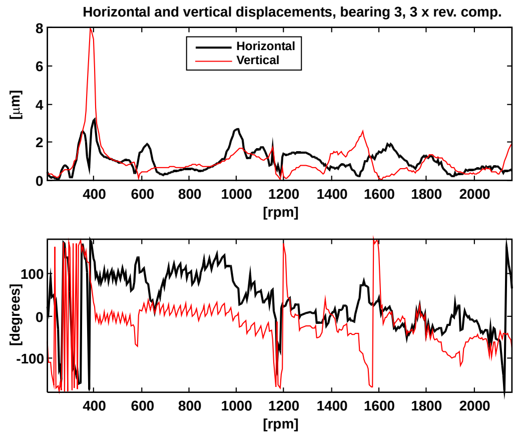

Figure 17 Experimental displacements at bearing 3, 3x rev. component of cracked shaft.

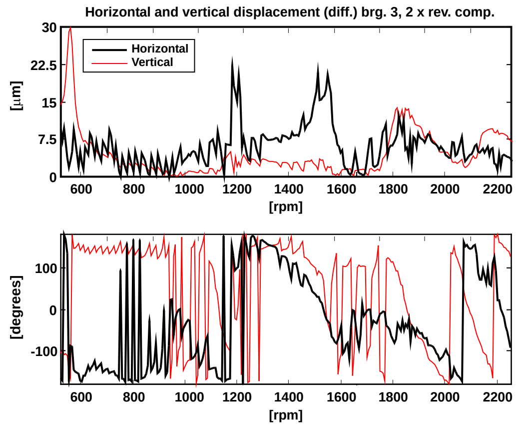

Figure 18 2x rev. vibration difference components at bearing 3.

Very high peaks are found in vertical direction when passing 1/2 critical speed for the 2x rev. component (Figure 19), and 1/3 critical speed for the 3x rev. component (Figure 20). Despite some 2x rev. excitations, due to journal ovalization, which is not accounted for in the model, and some 2x rev. and 3x rev. surface errors, a rather good agreement between calculated and measured results is generally found, which confirms the validity of the model. The measured 3x rev. component is heavily masked by 3x rev. surface errors (of roughly 5 μm).

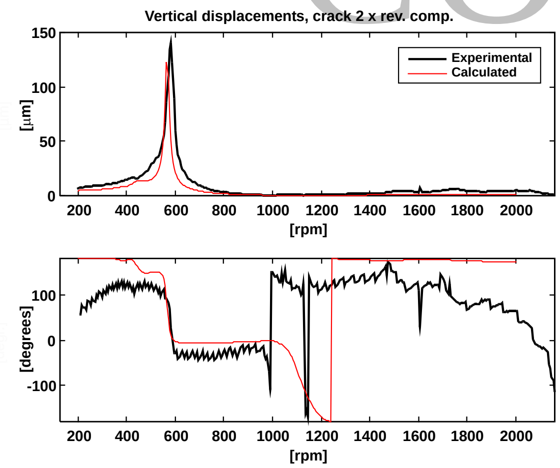

Figure 19 2x rev. measured and calculated vertical displacements at crack location.

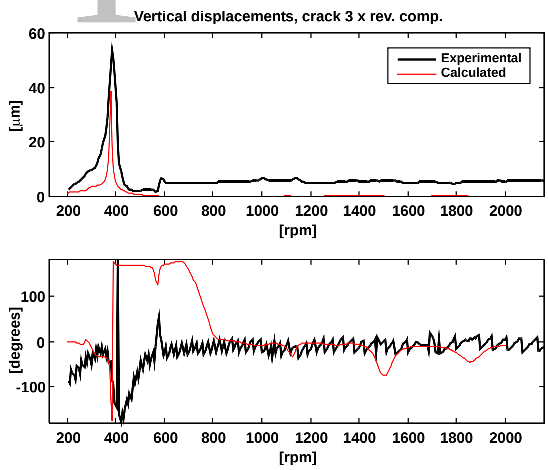

Figure 20 3x rev. measured and calculated vertical displacements at crack location

An attempt to identify the crack (its location and its amount) using only the “poor” bearing measurements (like those shown in Figure 18), considering separately the 2x rev. and 3x rev. components, lead to the results shown in Figure 21. The position of the identified crack is quite close to the actual position, both in 2x rev. and 3x rev. case, while the depth of the crack is overestimated. The poor quality of the identification is represented by the high values of the residual (δ = 0.859 and 0.923)

Neverthless this result can be deemed as good, considering the poor agreement between experimental and theoretical results, due to errors in processing the experimental data, and to the lack of experimental data in the lower speed range, where the 2x rev. and 3x rev. resonances amplify the corresponding vibration components. By considering also the measurements taken at crack location, which is unrealistic in plant operating machines, higher accuracy in location and depth is expected as shown for the 2x rev. component in Figure 22.

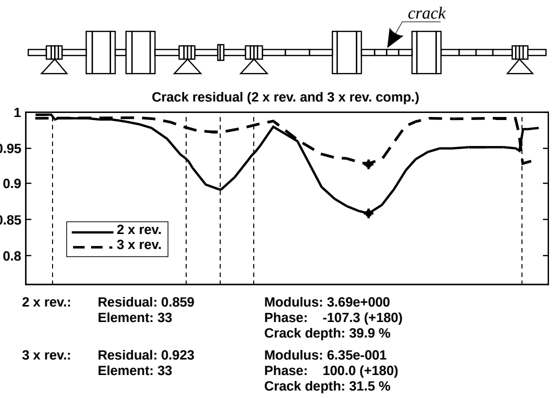

Figure 21 Identification of the crack with 2x rev. and 3x rev. components.

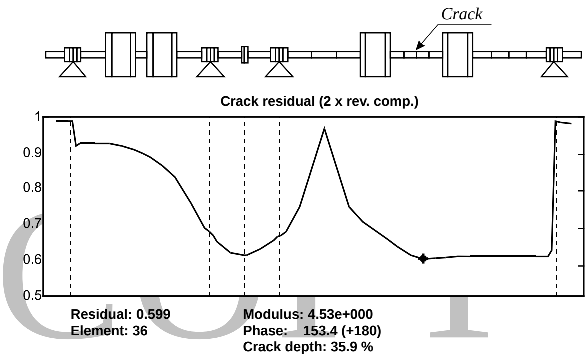

Figure 22 Identification of the crack with 2x rev. using also the measurements in the crack position.

CONCLUSIONS

In this paper, a model for the identification of both the location and the depth of a crack in a rotor has been presented. The least square identification method in the frequency domain has been used to determine the position of the crack and the equivalent bending moments due to the crack. The ratio of these bending moments to the static bending moment, in correspondence of the same element, due to the weight and to bearing alignment conditions, allows to determine the crack relative depth. The experimental data relative to both the static and dynamic behaviour of cracked rotor in a test-rig have been used to validate the proposed method.

ACKNOWLEDGEMENTS

This work is partially funded by the MURST (Italian Ministry for the University and Scientific Research) Cofinanziamento "IDENTIFICAZIONE DI MALFUNZIONAMENTI IN SISTEMI MECCANICI" for the year 1999.

REFERENCES

[1] Allianz, ALLIANZ Berichte, nr. 24 Nov. 1987, ISSN 0569-0692.

[2] Dimarogonas, A.D., "Vibration of cracked structures. A state of the art review", *Engineering Fracture Mechanics*, 55, 1996, pp.831-857.

[3] Bachschmid N., Pennacchi P., Tanzi E. and Audebert, S., "Identification of Transverse Cracks in Rotors Systems", Proc. of *ISROMAC-8 Conference*, 26-30 March 2000, Honolulu, Hawaii, ISBN 0-9652469-9-X, pp.1065-1072.

[4] Isermann R., "Fault Detection and Diagnosis: Methods and Applications", Proc. of *2nd International Symposium on Acoustical and Vibratory Surveillance Methods and Diagnostic Techniques*, CETIM, Senlis, October 1995.

[5] Bachschmid N., Pennacchi P., Tanzi E. e Vania A., "Accuracy of Modelling and Identification of Malfunctions in Rotor Systems: Experimental Results", *Journal of the Brazilian Society of Mechanical Sciences*, Vol. XXII, No 3, 2000, ISSN 0100-7386, pp. 423-442.

[6] Bachschmid N., Vania A., Tanzi E. e Pennacchi P., "Statical and Dynamical Behaviour of Rotors with Transversal Crack - Part I: Comparison between Different Models", Proc. of *XIV Congresso Nazionale AIMETA*, Como, 6-9 ottobre 1999.

NOMENCLATURE

$\mathbf{M}$, $\mathbf{D}$, $\mathbf{K}$	mass, damping and stiffness matrices of the rotor system (shaft + bearings + foundation);
$\mathbf{x}_t$	total vibration vector of the rotor system;
$\mathbf{F}(t)$	external force vector;
$\mathbf{x}$	vibration vector due to the developing fault;
$\mathbf{x}_1$	vibration vector due to weight and original unbalance;
$\mathbf{W}$	weight;
$M_u\, e^{i\Omega t}$	rotating original unbalance moment;
$U\, e^{i\Omega t}$	rotating original unbalance force;
$d\mathbf{M}$, $d\mathbf{D}$, $d\mathbf{K}$	mass, damping and stiffness matrices of the rotor system (shaft + bearings + foundation) changes due to fault;
$\mathbf{F}_f(t)$	fault force system vector;
$\mathbf{F}_{f_n}$	complex amplitude of the n^{th} harmonic component of $F_f(t)$;
$\mathbf{X}_n$	complex amplitude vector of the n^{th} harmonic component of x;
$\overline{A}$	complex amplitude of the fault equivalent generalized force;
$[\mathbf{F}_L]$	fault localisation vector;
Ω	rotating speed;
$[\mathbf{E}(n\Omega)]$	dynamic stiffness matrix for the n^{th} harmonic component;
$\boldsymbol{\alpha}_n$	inverse of $[\mathbf{E}(n\Omega)]$;
$\mathbf{X}_{A_n}$	complex amplitude vector of the n^{th} harmonic component of system vibrations except the journal displacements;
$\mathbf{X}_{B_n}$	complex amplitude vector of the n^{th} harmonic component of absolute journal displacements;
$\mathbf{X}_{Bm_n}$	complex amplitude vector of the n^{th} harmonic component of measured absolute journal displacements;
$\boldsymbol{\delta}_n$	complex residual of the identification procedure of the n^{th} harmonic component;
δ_{r_n}	relative residual of the identification procedure of the n^{th} harmonic component;
M	static bending moment;
M_n	n^{th} harmonic component of the bending moment due to a crack;
l	length of a element of the f.e.m.;

x_{st}	mean static deflection;
x_n	n^{th} harmonic component of the deflection;
l_c	length of the “equivalent” reduced stiffness element;
D	shaft diameter;
p	crack relative depth;